Accepted Manuscript

Title: Processable graphene oxide-embedded titanate nanofiber membranes with improved filtration performance

Author: Chao Xu Chen Wang Xiaoping He Miaoqiang Lyu Songcan Wang Lianzhou Wang

PII: S0304-3894(16)31127-X
DOI: http://dx.doi.org/doi:10.1016/j.jhazmat.2016.11.077
Reference: HAZMAT 18231

To appear in: *Journal of Hazardous Materials*

Received date: 27-6-2016
Revised date: 1-11-2016
Accepted date: 29-11-2016

Please cite this article as: Chao Xu, Chen Wang, Xiaoping He, Miaoqiang Lyu, Songcan Wang, Lianzhou Wang, Processable graphene oxide-embedded titanate nanofiber membranes with improved filtration performance, Journal of Hazardous Materials http://dx.doi.org/10.1016/j.jhazmat.2016.11.077

Processable graphene oxide-embedded titanate nanofiber membranes with improved filtration performance

Chao Xu [a,b,*], Chen Wang [a], Xiaoping He [a], Miaoqiang Lyu [b], Songcan Wang [b] and Lianzhou Wang [b,*]

[a] Research Institute of Photocatalysis, State Key Laboratory of Photocatalysis on Energy and Environment, Fuzhou University, Fuzhou 350002, P. R. China.

[b] School of Chemical Engineering and Australian Institute for Bioengineering and Nanotechnology, The University of Queensland, Brisbane, QLD. 4072, Australia.

*Corresponding author. Tel.: +86 591 83909068; fax: +86 591 83779105

Email address: cxu@fzu.edu.cn (C. Xu); l.wang@uq.edu.au (L.Z. Wang)

Graphical abstract

Processable graphene oxide-embedded titanate nanofiber membranes with improved filtration performance

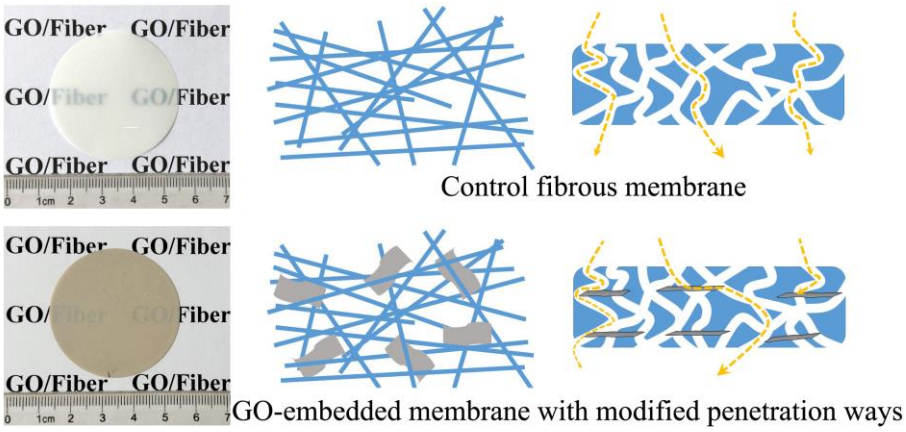

Highlights

- Graphene oxide embedded titanate fiber films with good processability are prepared
- The content of graphene oxide sheets and thickness of films can be adjusted easily
- Embedded graphene oxide sheets improve the filtration property of fibrous films
- Such composite films also exhibit enhanced selectivity performance.

Abstract

Graphene oxide (GO)-embedded titanate nanofiber (TNF) membranes with improved filtration performance are prepared successfully by a two-step method including electrostatic assembly of GO and TNFs into hybrids and subsequent processing of them into membranes by vacuum filtration. The embedded contents of GO sheets in films and thickness of as-assembled films can be adjusted facilely, endowing such composite films with good processability. Owing to the skilful introduction of GO sheets, the pore and/or channel structures in these hybrid membranes are modified. By treating different dye solutions (Direct Yellow and Direct Red), the filtration properties of these membranes show that the introduction of certain amount of GO sheets efficiently improve the separation performance of the membranes. Interestingly, these GO-embedded TNF membranes also display superior selective separation performance on filtrating the mixture solutions of such two dyes, making these hierarchical membranes more flexible and versatile in water treatment areas.

Keywords: Inorganic fibrous membranes, graphene oxide, processability, selectivity, water treatment

1. Introduction

Inorganic fibrous membranes have been considered as promising separation membranes due to their large surface area, high chemical and thermal stability, large porosity and high permeability, etc [1-4]. Despite of these advantages, the interconnected and open channels in fiber-based films are relatively large [5-8], which makes such membranes suffer a lot from poor retention efficiency and selectivity, limiting their potential applications in separation fields, especially in organic wastewater purification [9-12]. Generally, the permeation properties of fiber membranes can be improved by surface modification (for example, adsorption properties) [13, 14] and the structural adjustment of the pores/channels [15-17]. In addition to enhancing the adsorption capacity, modification of pore/channel structures could be an alternative and effective strategy to improve the retention ability of these films [18, 19]. Unfortunately, restricted by the fiber structures and the disorder assembling process of these fibers, the size of the as-formed pores (channels) in fibrous membranes are still hard to be well controlled. Thus, how to construct desirable pore/channel structures that could appropriately improve the separation performance of fibrous membranes is still a big challenge.

Graphene-based sheets have recently been found to be promising building blocks in film areas owing to their unique two-dimensional structure and properties [20-23]. Apart from used as the main components in films (sometime as surface coating membranes) [24-28], these carbon sheets have also been considered as excellent additives to improve certain properties of the films, for example conductivity, film-formation, antifouling and so on [29-31]. Thus, if these carbon sheets are successfully added into inorganic fibre filtration membranes, may the channels of membranes be modified, and their separation performance be improved [32-35]? As Scheme shown in Fig. 1, when carbon sheets are

introduced into fiber membranes, some of the interconnected and open channels in the as-obtained membranes may be segmented and cut off during the film assembly process, which would change the structure of these channels. Meanwhile, these embedded two-dimensional sheets could also increase the barrier area, which will delay substance permeation through the fiber membranes, improving the interception ability of these films. Accordingly, addition of graphene-based sheets could cause structural changes of these pores or channels in these inorganic fibrous films, which may affect the films' permeability and selectivity performance, resulting in improved filtration separation properties of these fibrous membranes.

Herein, we demonstrate a facile method to fabricate graphene oxide-embedded titanate ($H_2Ti_2O_7$) nanofiber (TNF) membranes with improved filtration separation properties. GO-embedded TNFs membranes are prepared by a two-step method including preparation of GO-$H_2Ti_2O_7$ nanofiber (TNF-GO) composites and assembling of them into membranes by simple vacuum filtration. The content of GO sheets and the thickness of films can also be adjusted facilely by our method. The separation performances of these GO embedded nanofibers membranes are investigated by filter organic dyes (Direct Yellow 50, Direct Red 80, or their mixed solutions). The results show that embedding GO sheets into these fiber membranes can efficiently improve the filtration separation performance of these TNF-GO membranes, which expands the potential applications of these hybrid filtration membranes in the film separation areas.

2. Experimental Section

2.1 Preparation of GO, TNF and TNF-GO composites

GO sheets were prepared from purified natural graphite (Alfa-Aesar Co.) according to the method reported by Hummers and Offeman [36]. Then the as-obtained GO dispersion (1 mg/ml) was sonicated and centrifuged to remove un-exfoliated and larger sheets. TNF are prepared using modified hydrothermal method according to the previous reports [34, 37]. First, tetra-n-butyl titanate (0.85 ml) was added in KOH solution (10 $mol \cdot L^{-1}$, 40 ml), which was stirred for 30 min to ensure a complete blending of the reactants. Then, the mixture was transferred to 50 mL Teflon-lined autoclave and was conducted at 200 ºC for 24 h. The product was collected after the hydrothermal reaction and washed using HCl (0.2 M) and deionized water to remove any impurities.

The as-obtained GO sheets and TNF are used as precursors to prepare TNF-GO composites. In a typical experiment, GO dispersion (0.25mL, 1 $mg \cdot mL^{-1}$) was added in titanate nanofibers suspension (50 mg of TNF dispersed in 50 mL of water) and the pH value was adjusted to around 6. Then, the as-formed slurry was stirred for 12 h at room temperature. Finally, the TNF-GO composites were centrifuged and washed with distilled water several times. Different usages of GO in TNF-GO composites were also prepared through the same process, and these samples are labelled as $TNF\text{-}GO_{x\%}$ (x %, mass ratios of original added GO sheets).

2.2 Film assembling and filtration test

Before membrane assembling, TNF and $TNF\text{-}GO_{x\%}$ composites (50 mg) were redispersed in HCl solution (0.2 M, 50 mL) for 2 days to form relatively stable suspensions. Then, TNF and TNF-GO membranes were prepared by vacuum filtration of the as-prepared suspensions through Poly(ether sulfones) filter membranes (47 mm in diameter, 0.2 μm pore size, Tianjin Jinteng). Distilled water was poured to wash these films. The filtration

properties of our membranes were evaluated by filtering different dye solutions, including Direct Yellow 50 (45 ppm), Direct Red 80 (35 ppm), and their mixture with the same concentrations. After washed by distilled water, 100 mL of these dye solution was poured on the top of the as-formed membranes, which was then subjected to continuous vacuum suction for 30 min (with a pressure of around 1 bar) to allow the solution to flow through the membranes. The volume of filtrate was recorded to calculate of flux for filtration membranes. The resultant filtrate was examined by ultraviolet-visible (UV-Vis) spectroscopy to calculate the relative concentration of filtrate (($C_{filtrate}/C_{feed}$) × 100 %) and retention rate ((1-$C_{filtrate}/C_{feed}$) × 100 %). Furthermore, the adsorption capacities of TNF and TNF-GO films were obtained by stirring the as-prepared films in the dye solution for 30 min. After centrifugation, the solution was analysed by UV-Vis spectroscopy ((1-$C_{adsorption}/C_{feed}$) × 100 %).

2.3 Characterization

Powder X-ray diffraction (XRD) analyses were performed on a Bruker D8 Advance diffractometer with Cu Kα radiation. The diffraction data were recorded for 2θ angles between 5o and 80^{o}. Thermogravimetric (TG) analyses were performed on NETZSCH thermogravimetric analyser from 15 to 800 ^{o}C at a heating rate of 5 ^{o}C /min in air flow. Morphology analyses of samples were carried out on JEOL 2100 Transmission Electron Microscope (TEM) and Hitachi S8010 Field Emission Scanning Electron Microscope (FESEM). The zeta-potential of samples and size of dye molecular was tested by Malvern Zetasizer Nano-ZS particle analyser. The UV-vis absorption spectra were carried out by Varian Cary 50 spectrophotometer. Specific surface areas and pore distribution were

calculated from nitrogen adsorption and desorption isotherms conducted at 77 K in an ASAP 2020 M analyser according to Brunauer-Emmett-Teller (BET) model.

3. Results and Discussion

3.1 Materials analysis

Fibers are usually utilized as starting materials to prepare bulk membranes [33, 38, 39]. To introduce GO sheets as effective additive in TNFs, we first prepared homogeneously TNF-$GO_{x\%}$ composites before processing them into membranes. It is found that the as-prepared TNFs carry positive charges under neutral and acidic condition, while GO sheets are usually negatively (the Zeta-potential values of TNF and GO suspension at pH 6 are about +29.8 and –30.4 mV, respectively) [40]. So TNF-$GO_{x\%}$ composites can be easily prepared by electrostatic assembly of two species with opposite chargers. Fig. 2(a) and (b) display typical TEM images of TNF control samples and TNF-$GO_{0.5\%}$ composites, respectively (Content of GO is confirmed by TGA results, Fig. S1, Supporting Information). From these figures, the typical fiber structure is clearly found, and the inset HRTEM image in Fig. 2(a) and XRD patterns (Fig. S2) indicate that these fibers possess titanate crystal structure. After electrostatic adsorption, TNFs are combined successfully with these carbon sheets, forming GO-involved TNF composites (as arrow shown in Fig. 2(b)) [41-43].

Generally, most of these inorganic nanofibers are in the form of powders or as precipitates from the solution, which are not feasible for these fibers to be processed into membranes by the post-synthesis assembly techniques. Dispersion assisting agents, especially polymer surfactants, are usually adopted to make inorganic fibers disperse more uniformly in aqueous solution [9, 10]. But these additives normally bring in some side-

effects, which would affect the inherent properties of these original nanofibers and the resulted fibrous membranes. Interestingly, in our cases, both TNF and TNF-$GO_{x\%}$ slurries can form relatively stable suspensions in acid solution (0.2 M HCl) without the addition of any dispersion agents, which remain for several hours without obvious precipitates (Insets in Fig. 3). Such phenomena are probably due to the strong electrostatic repulsion of these TNF-based fibers suspensions. As the insets shown in Fig. 3 (a) and (b), the Zeta-potential of TNF and TNF-$GO_{0.5\%}$ suspensions are about +42 and +33.6 mv, respectively, which make them disperse well in acid solution. Owing to such stability, these fiber materials show excellent membrane-formation properties, which can be readily assembled into film-like materials by vacuum filtration. Fig. 3 show the typical digital photos of TNF and TNF-$GO_{0.5\%}$ membranes (the usage of these fibers is about 50 mg.). It is clear that the assembled TNF films with certain transparency are very uniform, without using any surfactants (Fig. 3(a)) [33, 34]. By comparison, these TNF-$GO_{0.5\%}$ membranes become hazy with darker colour after introduction of these carbon sheets, but still look very homogeneous (Fig. S3). Furthermore, the disappearance of typical XRD patterns of GO flakes indicates that GO sheets are almost exfoliated in TNF membranes (Fig. S2).

The morphology of these films are analysed by FESEM images. Fig. 4 show the typical FESEM images of pure TNF and TNF-$GO_{0.5\%}$ membranes. It can be seen that TNF films are assembled by the inter-penetration and overlapping of these nanofibers [1-3], and the thickness of 50 mg TNF films is about 35 μm [33, 34]. After embedded with GO sheets, the surface structure of TNF-$GO_{0.5\%}$ membranes are similar to that of pristine TNF ones (Fig. 4(c)), but GO sheets can be clearly found in these TNF-$GO_{0.5\%}$ composite films (Fig. 4(d). Moreover, the presence of these carbon sheets in cross-section (as arrow shown in

Fig. 4(e)) further confirms that these GO sheets are indeed embedded in the films. Due to the introduction of carbon sheets, TNF-$GO_{0.5\%}$ films become slightly thicker than that of TNF ones, which is about 38 μm (Fig. 4(f)).

Actually, when the contents of GO are further increased from 0.5 to 2 wt%, the surface of TNF-GO membranes gradually become coarse, and the films are inclined to crack when the usage of GO is above 2 wt %. Such phenomenon may be due to the facts that excess addition of GO sheets could aggravate the local aggregation of these fibers in the resulted membranes [33], which can cause the hierarchical fiber films non-uniform during the film-forming process, leading to the formation of cracks (Fig. S4).

In addition to the controllable contents of GO sheets in films, the thickness of the as-obtained membranes in our system can also be adjusted by varying the dosage of composite fibers suspension. For example, when the dosage of fibers are about 30 (80) mg, the thickness of TNF- $GO_{0.5\%}$ membranes is around 23 (60) μm (Fig. S5). Though the thickness control is not very precise by filtration, such method is rather a simple and superior one for large-scale production of fiber membranes with adjustable thickness [44, 45]. Recently, Cao and co-authors have shown that graphene-involved titanate fiber membranes can form directly after one-step hydrothermal reaction [33, 34]. But, the as-formed composites tend to form monolith-like film materials, which restricts their convenient processing. In contrast, the superior processability with controllable content of carbon sheets and thickness of films in our work enable us to prepare membranes in a more flexible and adjustable fashion which are important for applications of these TNF-GO films.

Nitrogen adsorption-desorption analysis was conducted to investigate the specific surface areas and pore structure of the films (Fig. 5 and Fig. S6). Usually, the addition of graphene-based sheets would affect the specific surface area of certain materials. But in our samples, as the content of these sheets are very small, the specific surface area of TNF-$GO_{0.5\%}$ films (285 $m^2 \cdot g^{-1}$) is comparable to that of pure TNF ones (282 $m^2 \cdot g^{-1}$). From Fig. 5A(a), it is clear that the control TNF membranes exhibit a type H3 hysteresis loop, indicating the presence of mesopore structure. And the calculated average pore size of TNF membranes is about 15.3 nm (Fig. 5B(a)). After integrated with GO sheets, TNF-$GO_{x\%}$ films display similar mesopore structures, but with small decrease in pore size (Fig. 5 and Fig. S6, 12.5 nm). It is known that, the pores in these fiber membranes are derived from the overlapping and inter-penetration of fibres. So when these GO sheets are inserted, some of these original mesh-like pores may be segmented and/or blocked by these two-dimensional barriers (Fig. 1(b)) [46, 47], resulting in size decrease in these pores. When excess GO sheets were used (from 1 to 2 wt%), the average size of pores recovered slightly, which may be caused by the formation of cracks in films (Fig. S4).

3.2 Filtration performance

As separation membranes, small variation of pores/channels could cause changes in their separation and selectivity performance. Before carrying out filtration separation experiments, we simply tested the permeability of the TNF-$GO_{x\%}$ membranes by filtering pure water, and the results are listed in Table 1, Entry 1. It is found that when no GO sheets added, the water flux of 50 mg TNF membranes is about 102.9 $L \cdot h \cdot m^{-2}$. Noticeably, the pure water flux through these TNF-GO membranes (50 mg) decreased. In particular, when the content of GO is about 0.5 wt%, the TNF-$GO_{0.5\%}$ membranes display the lowest flux,

which is about 69.6 $L \cdot h \cdot m^{-2}$. So, addition of GO sheets can bring about certain influences on the permeation performance of these GO-embedded TNF membranes.

Analogously, it is assumed that the separation performance of these TNF-$GO_{x\%}$ membranes could be different from that of the pristine TNF ones. We utilized Direct Yellow 50 (DY) solutions as original feeds to evaluate the filtration performances of these films, and the results are shown in Fig. 6 and Table 1 (Entry 2 to 4). Fig. 6A displays UV-Vis absorbance and photos of filtrates obtained by vacuum filtrating DY dye solutions over our films. It can be intuitively seen that the filtrates obtained by using TNF-$GO_{x\%}$ as filtration membranes are clearer than that of TNF ones (Fig. 6A), suggesting that the use of GO sheets can improve the filtration separation abilities of TNF membranes towards DY dye. To further investigate the effects of these embedded GO sheets, we also calculate the adsorption capacities and retention rates of our films (Fig. 6B and Table 1)[48, 49]. Generally, the added GO sheets could increase the adsorption capacities of dye molecules by static and/or conjugation adsorption. However, the usages of GO are much low in our samples, and DY molecular are negatively charged in solution (about -33 mV), the adsorption capacity of TNF-GO films don't increase obviously. For example, when we mixed these film with 100 mL feed solution [50], the adsorption amount of TNF-$GO_{0.5\%}$ just increased from 6.3% of control TNF to 8.9% towards DY solutions. Noticeably, the whole retention rates of TNF-GO films increase remarkably. In particular, the retention rate of TNF-$GO_{0.5\%}$ membrane reaches to 93.1%, which is much higher than that of TNF membranes (55.8%). Accordingly, it is assumed that apart from increasing adsorption capacity, these embedded GO sheets primarily improve the interception abilities of these TNF filtration films.

We attributed such improvement of filtration performance to the variations of pore/channel structures of these GO-embedded TNF membranes (Fig. 1 and 7). As discussed above, these embedded GO sheets slightly reduce the average size of pores (Fig.5B and Fig. S6), which can narrow these interconnected channels in these GO-embedded films. And these inserted carbon sheets could seal up some channels (Fig. 7(b)). Thus, these narrowed and blocked channels are inclined to intercept more dye molecules (Fig. 7(b)). On the other hand, these GO sheets can increase the barrier area, which will improve the collision probability between pollutants and the membrane, and slow down the permeation rate of dye molecules through the films (Fig. 7(b)). Meanwhile, these two-dimensional sheets can also form local plane-liked channels (as the circular ring shown in Fig. 7(b)), which can further prolong the transferring route of these dye molecules. As results, these embedded carbon sheets can effectively improve the retention rate of these TNF-GO membranes towards dye molecules.

It should be noted that only certain amount of GO will facilitate the filtration process whereas further increasing the content of GO sheets (from 1 to 2 %) will not improve the retention rate, in reverse lead to a deterioration in their separation performance (Fig. 6 and Table 1, Entry 3). As discussed above, addition of excessive GO sheets may lead to the formation of cracks during the film-forming process (Fig. S4). Thus, dye molecules can permeate through these large voids and flow down with filtrates, which thereby reduces the retention rates of these TNF-$GO_{x\%}$ films. And probably due to the same reason, the fluxes (Table1, Entry 1 and 2) of these TNF membranes with excess GO sheets also exhibit similar variation tendency.

As known, the thickness of films has certain influence on the permeation performance [51, 52], so we chose TNF-$GO_{0.5\%}$ composites as model to further study the effects of membranes thickness on the filtration properties. Since the thickness of TNF-GO films can be controlled facilely just through using different amount of TNF-GO composites, three dosages of composites (30, 50 and 80 mg) are investigated and the corresponding TNF membranes are still used as control samples. From Fig. 8A, it can be seen that the retention rates of TNF and TNF-$GO_{0.5\%}$ membranes towards DY molecules are improved along with the increase in dosages of fibers, which may be caused by the increased adsorption capacities of films and the prolonged twisty channels in the films. But, no matter how the dosage of film adjusted, GO-embedded TNF membranes always display better retention rates than that of TNF ones. Usually, the thicker the films, the higher retention ability they possess, but worse in permeability. Thus, given the process cost, it is expected to obtain thinner membranes in the case of similar separation properties. It is found that, in our system, only 50 mg TNF-$GO_{0.5\%}$ membranes can achieve similar separation ability with that of 80 mg TNF films. Meanwhile, the flux of 50 mg TNF-$GO_{0.5\%}$ membranes also increase to 63.1 $L \cdot h \cdot m^{-2}$, compared with that of 80 mg pure TNF ones (56.8 $L \cdot h \cdot m^{-2}$), indicating that the relatively thin TNF-$GO_{0.5\%}$ membranes possess higher treatment capacity of wastewater in the case of similar retention rates.

Furthermore, we also found that these TNF-GO membranes display excellent separation performance on the other type of dyes. We use 30 mg films to filtrate direct red 80 solution (DR, 35 ppm, 100 mL), and the results indeed shown that GO-embedded TNF membranes exhibit enhanced filtration performance towards DR solution. Similarly, TNF-$GO_{0.5\%}$

membranes possess the highest retention rate (94.1%), which is about 1.4 times as that of control TNF ones. Accordingly, it is feasible that the filtration performance of these fiber membranes can be improved effectively by embedded with these two-dimensional sheets. And the controllable content of graphene oxide sheets and thickness of the films make them more flexible and versatile in water purification areas.

Apart from the enhanced retention performance, we also found that our films possess certain selectivity separation ability. As indicated in Fig.8, 30 mg TNF-$GO_{0.5\%}$ membranes can reject most DR dye molecules (Fig. 8B), but show poor retention rate on DY dye (Fig. 8A), so what is the result if using 30 mg films to filtrate the mixture of such two dyes? We preliminary test the selectively separation performance of these 30 mg TNF-$GO_{x\%}$ films on the mixture dye solution containing DY and DR dyes (100 mL with 45 ppm of DY and 35 ppm of DR), and Fig. 9 shows the relative concentration (($C_{filtrate}/C_{feed}$) × 100 %) of the two dyes in filtrates after vacuum filtration. As indicated in Fig. 9, when no GO sheets added, both of DY and DR dyes can permeate the pure TNF membranes, and the relative concentrations of DY and DR dyes in filtrates are about 95.1 and 35.7%, respectively. After embedded with GO sheets, most of DY dye molecules in the mixture can also permeate these TNF-$GO_{x\%}$ membranes easily, and the penetration rates of DY dye remain around 90%, which indicates that these embedded GO sheets have no significant effects on the selective penetration of DY dye in mixture system. Interestingly, the penetration rates of DR dye are influenced obviously by these added GO sheets. Particularly, the relative concentration of DR in filtrate through TNF-$GO_{0.5\%}$ membranes is only about 6.2%, which is much lower than that of using pure TNF samples (35.7%), suggesting that DR molecules in mixture can be selectively rejected by TNF-$GO_{0.5\%}$ membranes.

It is noteworthy that the conditions are more complex in mixture dye solution than that of single ones (such as concentration, adsorption properties, molecular weight, etc.), the filtration performance of TNF-GO membranes on such two dyes in mixture system are different from that of individual dye solution, which will be investigated in the future. Nevertheless, our results demonstrate that embedding with GO sheets can not only improve the filtration performance of TNF membranes, but also endows these films with exciting selectivity separation properties towards multi-component solutions, which could be utilized on some emerging applications such as petroleum industries, pharmaceuticals, food industries etc., opening up enormous opportunities for the use of graphene-involved fiber membranes in separation areas.

4. Conclusion

In summary, GO-embedded TNF membranes with improved filtration performance have been successfully obtained by a two-step method. First, TNF-$GO_{x\%}$ composites with controllable contents of GO sheets were prepared by electrostatic assembly from stable suspension. Then, TNF-$GO_{x\%}$ membranes were obtained by vacuum filtration of these suspensions. The thickness of these fiber membranes can also be facilely adjusted by changing the dosage of these stable fiber suspensions. The filtration properties of these TNF-GO membranes are evaluated by filtrating DY and DR dye solution. Since the introduction of these carbon sheets can modified the pore/channel structure of the original TNF films, the filtration performance of these GO-embedded TNF membranes is improved obviously. When the embedded amount of GO sheets is about 0.5 wt%, the composite membranes display the optimal separation properties towards these dyes. Furthermore, these TNF-GO membranes display superior selectivity separation properties towards the

mixture solutions of DY and DR dye, qualifying them as multi-functional membrane for separation applications.

It is assumed that such strategy that embedding graphene-based sheets into nanofiber membranes can be expanded to optimize the filtration properties of other inorganic fiber membranes, broadening the potential applications of these graphene-embedded inorganic fiber membranes in separation areas in the future.

Acknowledgment

This work was financially supported by the Independent Research Project of State Key Laboratory of Photocatalysis on Energy and Environment (2014B04), the program for Qishan Scholar in Fuzhou University, and the National Key Technologies R & D Program of China (2014BAC13B03)

References:

[1] Q.Y. Xu, M.A. Anderson, Synthesis of Porosity Controlled Ceramic Membranes, J. Mater. Res. 6 (1991) 1073-1081.

[2] X.B. Ke, H.Y. Zhu, X.P. Gao, J.W. Liu, Z.F. Zheng, High-performance ceramic membranes with a separation layer of metal oxide nanofibers, Adv. Mater. 19 (2007) 785-790.

[3] X.S. Peng, J. Jin, E.M. Ericsson, I. Ichinose, General method for ultrathin free-standing films of nanofibrous composite materials, J. Am. Chem. Soc. 129 (2007) 8625-8633.

[4] M.M. Wang, J. Song, X.R. Wu, X.Y. Tan, B. Meng, S.M. Liu, Metallic nickel hollow fiber membranes for hydrogen separation at high temperatures, J. Membr. Sci. 509 (2016) 156-163.

[5] D.S. Sholl, J.K. Johnson, Making high-flux membranes with carbon nanotubes, Science 312 (2006) 1003-1004.

[6] J.K. Yuan, X.G. Liu, O. Akbulut, J.Q. Hu, S.L. Suib, J. Kong, F. Stellacci, Superwetting nanowire membranes for selective absorption, Nat. Nanotechnol. 3 (2008) 332-336.

[7] H.-W. Liang, L. Wang, P.-Y. Chen, H.-T. Lin, L.-F. Chen, D. He, S.-H. Yu, Carbonaceous Nanofiber Membranes for Selective Filtration and Separation of Nanoparticles, Adv. Mater. 22 (2010) 4691-4695.

[8] H.R. Pant, H.J. Kim, M.K. Joshi, B. Pant, C.H. Park, J.I. Kim, K.S. Hui, C.S. Kim, One-step fabrication of multifunctional composite polyurethane spider-web-like nanofibrous membrane for water purification, J. Hazard. Mater. 264 (2014) 25-33.

[9] Q. Yu, Y.Y. Mao, X.S. Peng, Separation Membranes Constructed from Inorganic Nanofibers by Filtration Technique, Chem. Rec. 13 (2013) 14-27.

[10] X.W. Zhang, T. Zhang, J. Ng, D.D. Sun, High-Performance Multifunctional TiO2 Nanowire Ultrafiltration Membrane with a Hierarchical Layer Structure for Water Treatment, Adv. Funct. Mater. 19 (2009) 3731-3736.

[11] Q. Wen, J.C. Di, Y. Zhao, Y. Wang, L. Jiang, J.H. Yu, Flexible inorganic nanofibrous membranes with hierarchical porosity for efficient water purification, Chem. Sci. 4 (2013) 4378-4382.

[12] X.S. Peng, I. Ichinose, Green-Chemical Synthesis of Ultrathin beta-MnOOH Nanofibers for Separation Membranes, Adv. Funct. Mater. 21 (2011) 2080-2087.

[13] H.W. Liang, X. Cao, W.J. Zhang, H.T. Lin, F. Zhou, L.F. Chen, S.H. Yu, Robust and Highly Efficient Free-Standing Carbonaceous Nanofiber Membranes for Water Purification, Adv. Funct. Mater. 21 (2011) 3851-3858.

[14] P. Chen, H.-W. Liang, X.-H. Lv, H.-Z. Zhu, H.-B. Yao, S.-H. Yu, Carbonaceous Nanofiber Membrane Functionalized by beta-Cyclodextrins for Molecular Filtration, Acs Nano 5 (2011) 5928-5935.

[15] S. Yang, Y. Si, Q.X. Fu, F.F. Hong, J.Y. Yu, S.S. Al-Deyab, M. El-Newehy, B. Ding, Superwetting hierarchical porous silica nanofibrous membranes for oil/water microemulsion separation, Nanoscale 6 (2014) 12445-12449.

[16] X. Li, M. Wang, C. Wang, C. Cheng, X.F. Wang, Facile Immobilization of Ag Nanocluster on Nanofibrous Membrane for Oil/Water Separation, ACS Appl. Mat. Interfaces 6 (2014) 15272-15282.

[17] Y.E. Miao, R.Y. Wang, D. Chen, Z.Y. Liu, T.X. Liu, Electrospun Self-Standing Membrane of Hierarchical SiO2@gamma-AlOOH (Boehmite) Core/Sheath Fibers for Water Remediation, ACS Appl. Mat. Interfaces 4 (2012) 5353-5359.

[18] X. Zhang, C. Cheng, J. Zhao, L. Ma, S. Sun, C. Zhao, Polyethersulfone enwrapped graphene oxide porous particles for water treatment, Chem. Eng. J. 215 (2013) 72-81.

[19] C. Wang, J. Zhou, J. Ni, Y. Cheng, H. Li, Design and synthesis of pyrophosphate acid/graphene composites with wide stacked pores for methylene blue removal, Chem. Eng. J. 253 (2014) 130-137.

[20] W. Hu, C. Peng, W. Luo, M. Lv, X. Li, D. Li, Q. Huang, C. Fan, Graphene-Based Antibacterial Paper, Acs Nano 4 (2010) 4317-4323.

[21] H.M. Hegab, L.D. Zou, Graphene oxide-assisted membranes: Fabrication and potential applications in desalination and water purification, J. Membr. Sci. 484 (2015) 95-106.

[22] X.N. Zhao, P.P. Zhang, Y.T. Chen, Z.Q. Su, G. Wei, Recent advances in the fabrication and structure-specific applications of graphene-based inorganic hybrid membranes, Nanoscale 7 (2015) 5080-5093.

[23] L. Huang, M. Zhang, C. Li, G.Q. Shi, Graphene-Based Membranes for Molecular Separation, J. Phys. Chem. Lett. 6 (2015) 2806-2815.

[24] S.-Y. Huang, G.-P. Wu, C.-M. Chen, Y. Yang, S.-C. Zhang, C.-X. Lu, Electrophoretic deposition and thermal annealing of a graphene oxide thin film on carbon fiber surfaces, Carbon 52 (2013) 613-616.

[25] Y. Zhang, S. Zhang, T.S. Chung, Nanometric Graphene Oxide Framework Membranes with Enhanced Heavy Metal Removal via Nanofiltration, Environ. Sci. Technol. 49 (2015) 10235-10242.

[26] G. Wei, Y.-E. Miao, C. Zhang, Z. Yang, Z. Liu, W.W. Tjiu, T. Liu, Ni-Doped Graphene/Carbon Cryogels and Their Applications As Versatile Sorbents for Water Purification, ACS Appl. Mat. Interfaces 5 (2013) 7584-7591.

[27] P. Tan, J. Sun, Y.Y. Hu, Z. Fang, Q. Bi, Y.C. Chen, J.H. Cheng, Adsorption of Cu2+, Cd2+ and Ni2+ from aqueous single metal solutions on graphene oxide membranes, J. Hazard. Mater. 297 (2015) 251-260.

[28] G.E. Romanos, C.P. Athanasekou, F.K. Katsaros, N.K. Kanellopoulos, D.D. Dionysiou, V. Likodimos, P. Falaras, Double-side active TiO2-modified nanofiltration

membranes in continuous flow photocatalytic reactors for effective water purification, J. Hazard. Mater. 211 (2012) 304-316.

[29] J. Lee, H.-R. Chae, Y.J. Won, K. Lee, C.-H. Lee, H.H. Lee, I.-C. Kim, J.-m. Lee, Graphene oxide nanoplatelets composite membrane with hydrophilic and antifouling properties for wastewater treatment, J. Membr. Sci. 448 (2013) 223-230.

[30] S. Stankovich, D.A. Dikin, G.H.B. Dommett, K.M. Kohlhaas, E.J. Zimney, E.A. Stach, R.D. Piner, S.T. Nguyen, R.S. Ruoff, Graphene-based composite materials, Nature 442 (2006) 282-286.

[31] S. Bano, A. Mahmood, S.J. Kim, K.H. Lee, Graphene oxide modified polyamide nanofiltration membrane with improved flux and antifouling properties, J. Mater. Chem.A 3 (2015) 2065-2071.

[32] D.D. Xu, Q. Xu, K.X. Wang, J. Chen, Z.M. Chen, Fabrication of Free-Standing Hierarchical Carbon Nanofiber/Graphene Oxide/Polyaniline Films for Supercapacitors, ACS Appl. Mat. Interfaces 6 (2014) 200-209.

[33] L. Zhu, L. Gu, Y. Zhou, S. Cao, X. Cao, Direct production of a free-standing titanate and titania nanofiber membrane with selective permeability and cleaning performance, J. Mater. Chem. 21 (2011) 12503-12510.

[34] X.B. Cao, Y. Zhou, J. Wu, Y.X. Tang, L.W. Zhu, L. Gu, Self-assembled, robust titanate nanoribbon membranes for highly efficient nanosolid capture and molecule discrimination, Nanoscale 5 (2013) 3486-3495.

[35] T. Zhang, J. Liu, D.D. Sun, A novel strategy to fabricate inorganic nanofibrous membranes for water treatment: use of functionalized graphene oxide as a cross linker, RSC Adv. 2 (2012) 5134-5137.

[36] W.S. Hummers, R.E. Offeman, Preparation of graphitic oxide, J. Am. Chem. Soc. 80 (1958) 1339-1339.

[37] X.W. Zhang, A.J. Du, P.F. Lee, D.D. Sun, J.O. Leckie, TiO2 nanowire membrane for concurrent filtration and photocatalytic oxidation of humic acid in water, J. Membr. Sci. 313 (2008) 44-51.

[38] L. Shang, B.J. Li, W.J. Dong, B.Y. Chen, C.R. Li, W.H. Tang, G. Wang, J. Wu, Y.B. Ying, Heteronanostructure of Ag particle on titanate nanowire membrane with enhanced photocatalytic properties and bactericidal activities, J. Hazard. Mater. 178 (2010) 1109-1114.

[39] H.M. Zhang, H.J. Zhao, P.R. Liu, S.Q. Zhang, G.Y. Li, Direct growth of hierarchically structured titanate nanotube filtration membrane for removal of waterborne pathogens, J. Membr. Sci. 343 (2009) 212-218.

[40] D. Li, M.B. Muller, S. Gilje, R.B. Kaner, G.G. Wallace, Processable aqueous dispersions of graphene nanosheets, Nat. Nanotechnol. 3 (2008) 101-105.

[41] X. Pan, Y. Zhao, S. Liu, C.L. Korzeniewski, S. Wang, Z. Fan, Comparing Graphene-TiO2 Nanowire and Graphene-TiO2 Nanoparticle Composite Photocatalysts, ACS Appl. Mat. Interfaces 4 (2012) 3944-3950.

[42] G.M. Zhou, Y.B. Zhao, C.X. Zu, A. Manthiram, Free-standing TiO2 nanowire-embedded graphene hybrid membrane for advanced Li/dissolved polysulfide batteries, Nano Energy 12 (2015) 240-249.

[43] Q. Sun, S.J. Lee, H. Kang, Y. Gim, H.S. Park, J.H. Cho, Positively-charged reduced graphene oxide as an adhesion promoter for preparing a highly-stable silver nanowire film, Nanoscale 7 (2015) 6798-6804.

[44] J. Jin, Y. Wakayama, X. Peng, I. Ichinose, Surfactant-assisted fabrication of free-standing inorganic sheets covering an array of micrometre-sized holes, Nat. Mater. 6 (2007) 686-691.

[45] D.A. Dikin, S. Stankovich, E.J. Zimney, R.D. Piner, G.H.B. Dommett, G. Evmenenko, S.T. Nguyen, R.S. Ruoff, Preparation and characterization of graphene oxide paper, Nature 448 (2007) 457-460.

[46] F. Guo, G. Silverberg, S. Bowers, S.-P. Kim, D. Datta, V. Shenoy, R.H. Hurt, Graphene-Based Environmental Barriers, Environ. Sci. Technol. 46 (2012) 7717-7724.

[47] K.L. Goh, L. Setiawan, L. Wei, R.M. Si, A.G. Fane, R. Wang, Y. Chen, Graphene oxide as effective selective barriers on a hollow fiber membrane for water treatment process, J. Membr. Sci. 474 (2015) 244-253.

[48] T.S. Sreeprasad, S. Sen Gupta, S.M. Maliyekkal, T. Pradeep, Immobilized graphene-based composite from asphalt: Facile synthesis and application in water purification, J. Hazard. Mater. 246 (2013) 213-220.

[49] J.R. Ellerie, O.G. Apul, T. Karanfil, D.A. Ladner, Comparing graphene, carbon nanotubes, and superfine powdered activated carbon as adsorptive coating materials for microfiltration membranes, J. Hazard. Mater. 261 (2013) 91-98.

[50] L. Huang, J. Chen, T. Gao, M. Zhang, Y. Li, L. Dai, L. Qu, G. Shi, Reduced Graphene Oxide Membranes for Ultrafast Organic Solvent Nanofiltration, Adv. Mater. 28 (2016) 8669-8674.

[51] J.W. Liu, H.W. Liang, S.H. Yu, Macroscopic-Scale Assembled Nanowire Thin Films and Their Functionalities, Chem. Rev. 112 (2012) 4770-4799.

[52] P. Vandezande, L.E.M. Gevers, I.F.J. Vankelecom, Solvent resistant nanofiltration: separating on a molecular level, Chem. Soc. Rev. 37 (2008) 365-405.

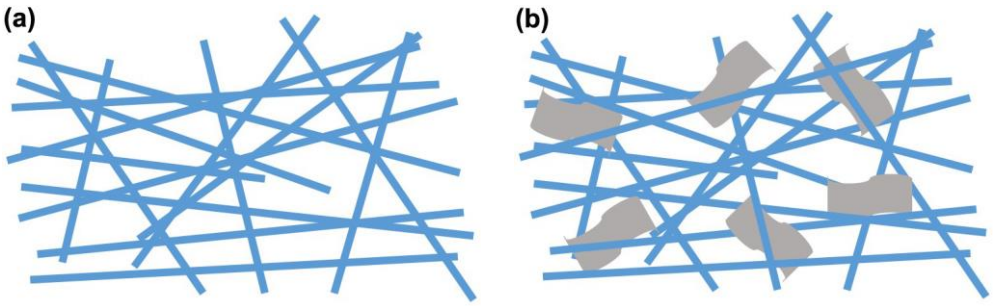

Fig. 1. Scheme of (a) pure fiber membranes and (b) GO-embedded fiber membranes.

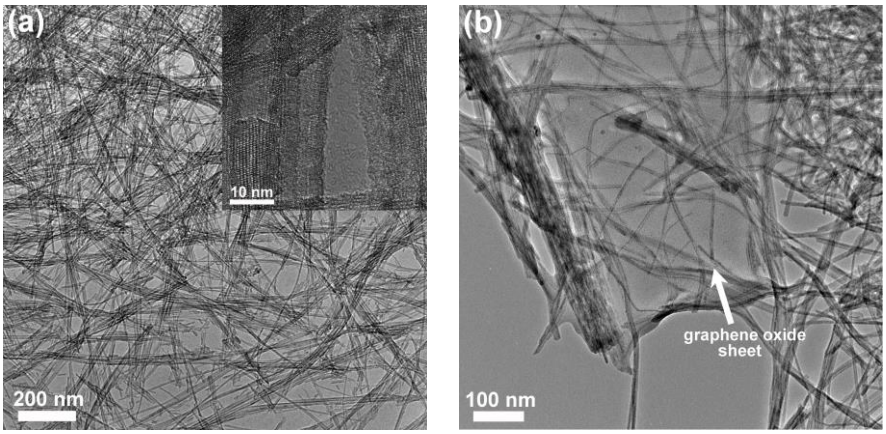

Fig. 2. TEM images of (a) TNF and (b) TNF-$GO_{0.5\%}$ membranes. Inset in (a) is the HRTEM image of titanate fibers.

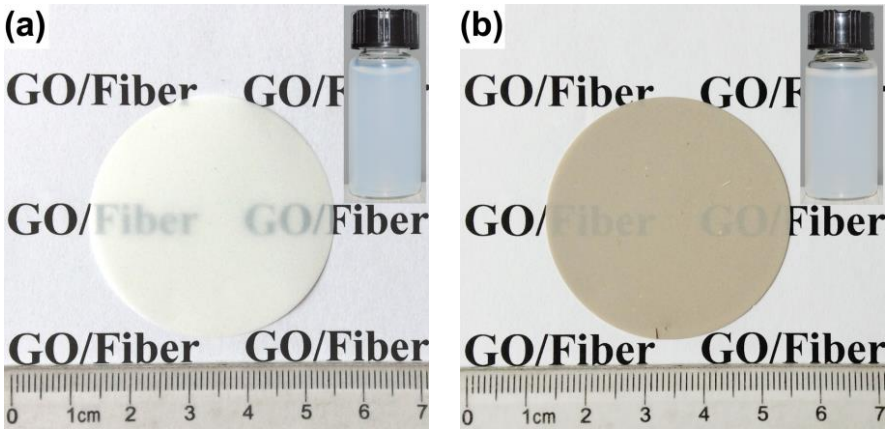

Fig. 3. Digital photos of (a) TNF and (b) TNF-$GO_{0.5\%}$ membranes, and the dosage of fibers is about 50 mg. Insets are photos of corresponding suspensions of fiber materials (1.0 mg/mL).

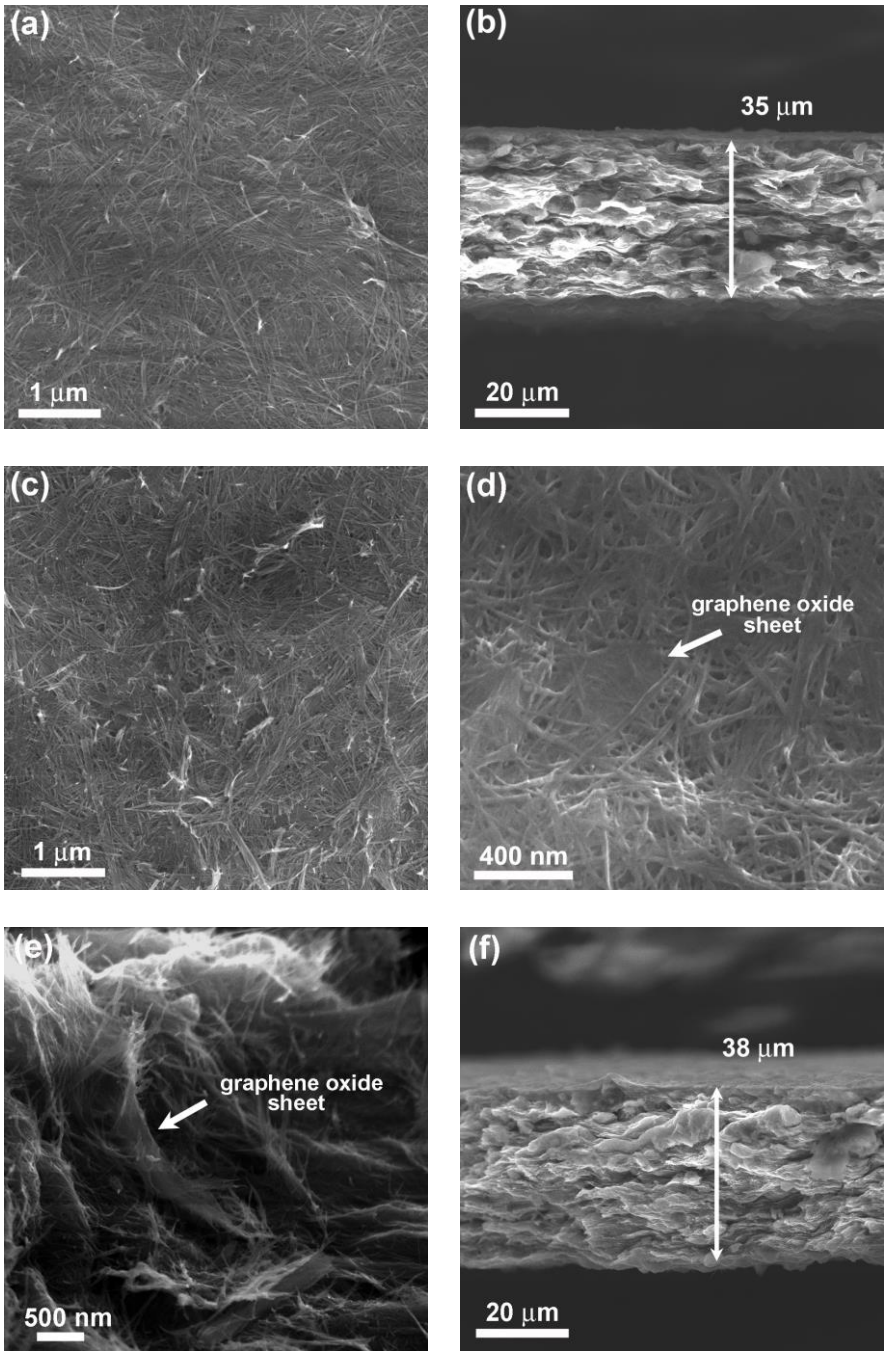

Fig. 4. FESEM images of samples: (a) and (b) TNF membranes, (c) and (d) TNF-$GO_{0.5\%}$ membranes.

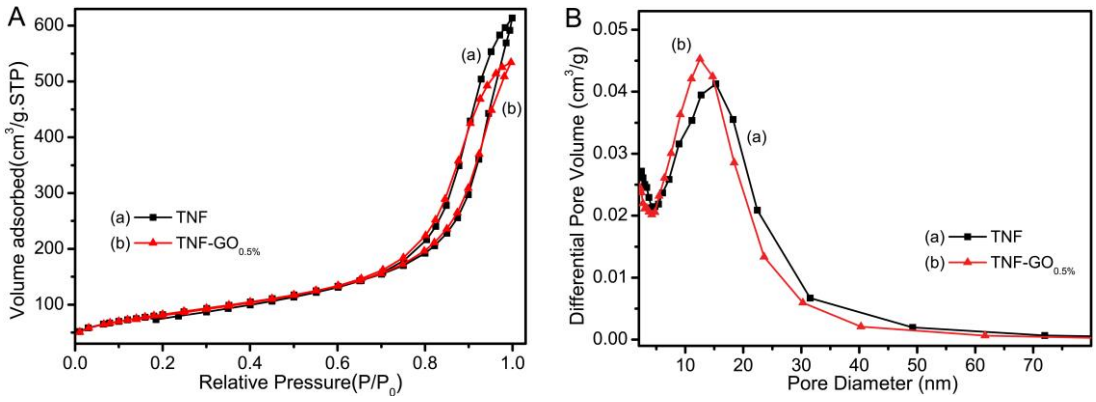

Fig. 5. (A) Nitrogen adsorption-desorption isotherms and (B) pore size distribution curve of (a) TNF and (b) TNF-$GO_{0.5\%}$ membranes.

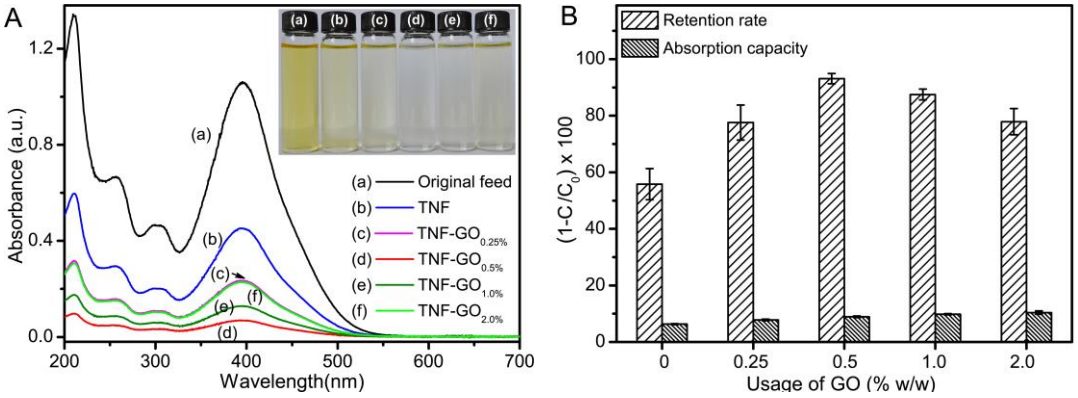

Fig. 6. (A) UV-Vis absorbance and photos of filtrates obtained by filtration of DY solutions for 30 min (45 ppm, 100 ml) over 50 mg TNF and TNF-GO membranes; (B) Bar plot showing the retention rates and adsorption capacities of these membranes. Retention rate = $(1 - C_{filtrate}/C_{feed}) \times 100$ %, and adsorption capacity = $(1 - C_{adsorption}/C_{feed}) \times 100$ %.

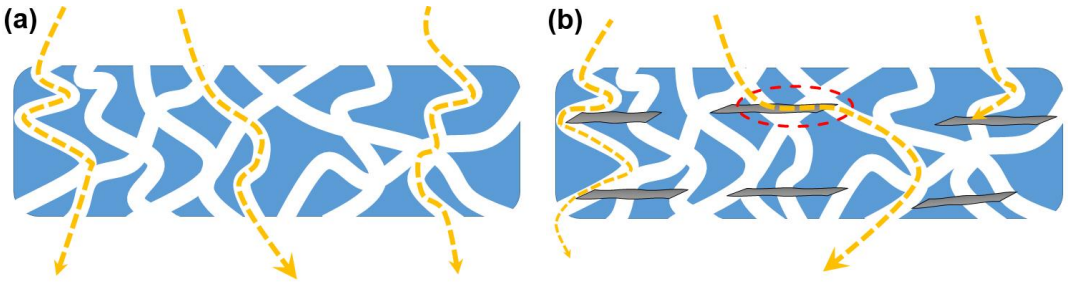

Fig. 7. Schematic view for possible percolation through the fiber membranes (a) TNF and (b) TNF-GO filtration membranes.

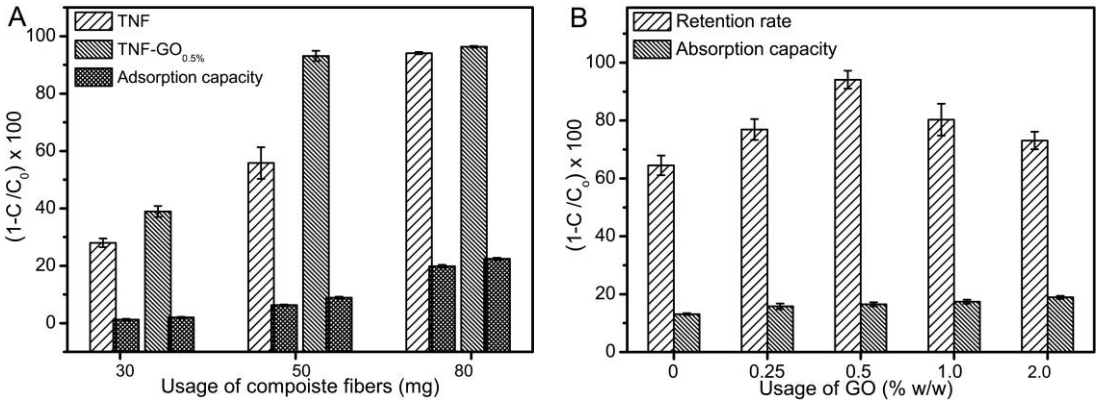

Fig. 8. (A) The retention rates and adsorption capacities of DY solution (45 ppm, 100 mL) using different usage of TNF and TNF-$GO_{0.5\%}$ membranes. (B) The retention rates and adsorption capacities of DR solution (35 ppm, 100 mL) using 30 mg membranes with different usage of GO sheets.

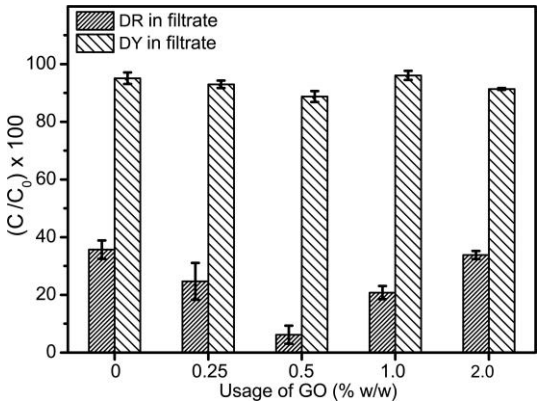

Fig. 9. Concentration of DY and DR dyes in filtrates using 30 mg of membranes with different contents of GO sheets. Relative concentration = ($C_{filtrate}/C_{feed}$) × 100 %.

Table 1. Flux, retention rate and adsorption parameters obtained by using 50 mg membranes with different content of GO sheets. The volume of feeds is 100 mL (pure water or 45 ppm of DY dye), and the filtration time is 30 min.

Entry	Usage of GO (wt %)	0	0.25	0.5	1.0	2.0
1	Pure water flux ($L \cdot h \cdot m^{-2}$)	102.9±0.4	89.9±0.4	69.6±0.3	80.6±0.4	86.6±0.4
2	Dye solution flux ($L \cdot h \cdot m^{-2}$)	95.8±6.7	79.0±3.8	63.1±3.6	76.1±6.9	81.4±8.0
3	Retention rate (%)	55.8±5.5	77.6±6.2	93.1±1.8	87.5±1.9	77.9±4.6
4	Adsorption capacity (%)	6.3±0.2	7.8±0.3	8.9±0.3	9.8±0.2	10.4±0.6